

Provided for non-commercial research and education use.  
Not for reproduction, distribution or commercial use.



This article appeared in a journal published by Elsevier. The attached copy is furnished to the author for internal non-commercial research and education use, including for instruction at the authors institution and sharing with colleagues.

Other uses, including reproduction and distribution, or selling or licensing copies, or posting to personal, institutional or third party websites are prohibited.

In most cases authors are permitted to post their version of the article (e.g. in Word or Tex form) to their personal website or institutional repository. Authors requiring further information regarding Elsevier's archiving and manuscript policies are encouraged to visit:

<http://www.elsevier.com/copyright>



Contents lists available at ScienceDirect

Catalysis Today

journal homepage: [www.elsevier.com/locate/cattod](http://www.elsevier.com/locate/cattod)

## Study on Pt/Al-MCM-41 for NO selective reduction by hydrogen

Peng Wu<sup>a,b</sup>, Landong Li<sup>a,\*</sup>, Qing Yu<sup>a</sup>, Guangjun Wu<sup>a</sup>, Naijia Guan<sup>a</sup><sup>a</sup> Key Laboratory of Functional Polymer Materials, Ministry of Education & Institute of New Catalytic Materials Science, College of Chemistry, Nankai University, Weijin Road 94#, Tianjin 300071, China<sup>b</sup> China Shenhua Coal to Liquid and Chemical Beijing Research Institute, Beijing 100011, PR China

### ARTICLE INFO

#### Article history:

Available online 8 April 2010

#### Keywords:

H<sub>2</sub>-SCR  
Brønsted acid  
Pt/Al-MCM-41

### ABSTRACT

Al species can be introduced to the framework of Si-MCM-41 support by isomorphous substitution or wet impregnation and Brønsted acid sites can be created in Al-MCM-41. Pt catalysts supported on Si-MCM-41 and Al-MCM-41 are studied for the selective catalytic reduction of NO by hydrogen in excess oxygen. The introduction of Al species to MCM-41 at suitable Si/Al ratio shows great promotion effect on H<sub>2</sub>-SCR over Pt/MCM-41. Pt catalyst supported on Al-MCM-41 prepared by isomorphous substitution with the Si/Al ratio of 10 exhibits the best catalytic performance and ca. 80% NO<sub>x</sub> conversion as well as ca. 85% N<sub>2</sub> selectivity can be achieved at 140 °C at high GHSV of 80,000 h<sup>-1</sup>. The H<sub>2</sub>-SCR reaction over Pt/Al-MCM-41, together with Pt/Si-MCM-41, are investigated by means of in situ DRIFT spectra and the existence of Brønsted acid sites in Al-MCM-41 is found to play a decisive role on the H<sub>2</sub>-SCR reaction pathway.

© 2010 Elsevier B.V. All rights reserved.

### 1. Introduction

Catalytic elimination of nitrogen oxides (NO<sub>x</sub>) is always a hot topic in the field of environmental catalysis. Selective catalytic reduction of NO<sub>x</sub> by ammonia (NH<sub>3</sub>-SCR) is a well-known process for NO<sub>x</sub> emissions control and has been successfully applied in the post-treatment of NO<sub>x</sub> from stationary sources [1]. Recently, hydrogen has been proved to be effective reductant for NO<sub>x</sub> reduction even in excess oxygen over a series of catalysts [2–13]. It is desirable to replace ammonia with less processed and less expensive nontoxic hydrogen in the SCR process. Therefore, selective catalytic reduction of nitrogen oxides by hydrogen (H<sub>2</sub>-SCR) is studied as possible alternative for NH<sub>3</sub>-SCR.

In the research of possible H<sub>2</sub>-SCR catalysts, noble metal catalysts, e.g. Pt catalysts [2–9] and Pd catalysts [10–12], have received considerable attention due to their high activities at low temperatures ( $T < 200$  °C). For Pt catalysts, it is found that the activity and selectivity are strongly influenced by the properties of support materials. On the one side, acidic supports, e.g. zeolites with Brønsted acid sites, are helpful to stabilize active metallic Pt and to store ammonia as intermediate for SCR process [7]. As a result, high SCR activity and high N<sub>2</sub> selectivity are achieved on Pt catalysts on acidic supports. On the other side, basic supports with Lewis base sites favor the adsorption of NO<sub>2</sub><sup>-</sup>-type species as intermediates for SCR process and high SCR activity as well as high N<sub>2</sub> selectivity

is also achieved on Pt catalysts on basic supports [8]. Obviously, different adsorption species are observed as intermediates during H<sub>2</sub>-SCR reaction on different Pt catalysts, and correspondingly, different H<sub>2</sub>-SCR pathways are involved in the reaction. Mesoporous MCM-41 has been successfully applied as high-surface-area supports for HC-SCR catalysts [14,15]. In our previous work, Pt catalysts supported on mesoporous Si-MCM-41 exhibits much better activity in H<sub>2</sub>-SCR reaction than Pt/silicate and Pt/SiO<sub>2</sub> [16]. The mesoporous structure of Si-MCM-41 support is found to be essential to achieve the high activity. However, as we know, Si-MCM-41 is a neutral support without Brønsted acid sites or Lewis base sites. Therefore, the introduction of Brønsted acid sites or Lewis base sites to Si-MCM-41 may be possible means to enhance the SCR activity and N<sub>2</sub> selectivity of Pt/Si-MCM-41.

In the present study, Al species are introduced to Si-MCM-41 support by isomorphous substitution or wet impregnation and Al-MCM-41 with Brønsted acid sites are obtained. The catalytic performance of Pt/Al-MCM-41 is investigated for H<sub>2</sub>-SCR reaction and the promotion effect of Al species is studied. Moreover, the H<sub>2</sub>-SCR reaction pathways on Pt/Al-MCM-41 and Pt/Si-MCM-41 are investigated by means of in situ DRIFT spectra.

### 2. Experimental

#### 2.1. Catalyst preparation

Mesoporous Si-MCM-41 sample was prepared by a hydrothermal route with cetyltrimethylammonium bromide (CTAB) as template and the details can be found in our previous work [16]. The

\* Corresponding author.

E-mail address: [lild@nankai.edu.cn](mailto:lild@nankai.edu.cn) (L. Li).

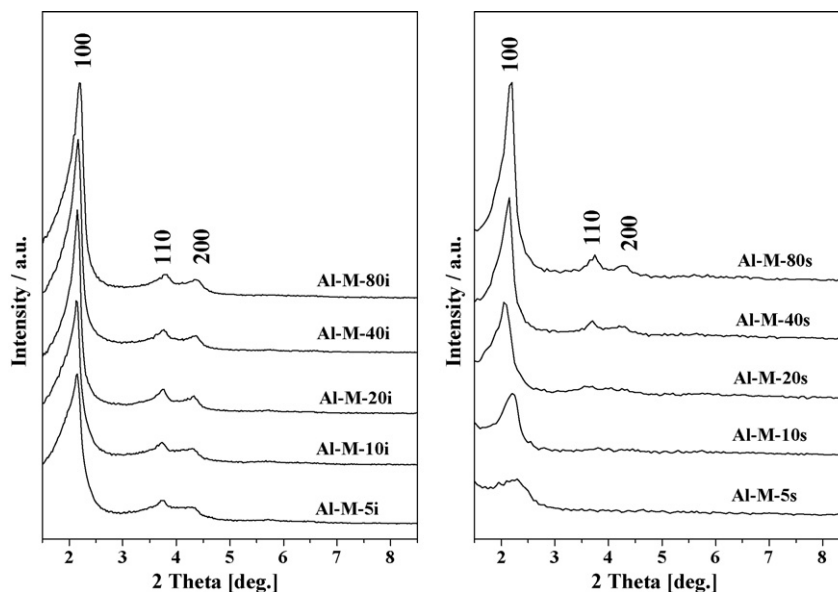


Fig. 1. XRD patterns of Al-MCM-41 prepared by different methods.

Al-MCM-41 samples were prepared by isomorphous substitution and wet impregnation. For isomorphous substitution, a hydrothermal route similar to the synthesis of Si-MCM-41 was employed. Briefly, CTAB, tetraethyl orthosilicate (TEOS) and  $\text{Al}_2(\text{SO}_4)_3$  were slowly added into distilled water in turn under stirring and the pH value of obtained gel was adjusted to *ca.* 10.5. After further stir at 60 °C for 4 h, the gel was transported into an autoclave for crystallization at 110 °C for 12 h. The resulted solid was filtered, washed, dried at 80 °C and calcined at 500 °C. The product was defined as Al-M-*x*s, in which *x* indicating the Si/Al ratio. For wet impregnation, 1 g MCM-41 was impregnated with 5 mL  $\text{Al}(\text{NO}_3)_3$  solution. The slurry was evaporated under stirring at 80 °C and then calcined in air at 500 °C. The final product was defined as Al-M-*x*i, in which *x* indicating the Si/Al ratio.

Pt catalysts on different supports with Pt loading of *ca.* 1% were prepared by incipient wetness impregnation method, using potassium chloroplatinate as platinum precursor. The catalysts were dried at 80 °C for 12 h and then calcined in air at 400 °C for 3 h.

## 2.2. Catalyst characterization

Powder X-ray diffraction (XRD) measurements were performed on the samples using a Rigaku D/max 2500 diffractometer, equipped with a graphite monochromator and using  $\text{Cu K}\alpha$  radiation.

The textural properties of samples were analyzed by low temperature  $\text{N}_2$  adsorption/desorption using a Quantachrome NOVA-1200 gas absorption analyzer and the specific surface areas were calculated using the BET equation.

Transmission electron microscopy (TEM) images of samples were acquired on a Tecnai G<sup>2</sup> 2010 S-TWIN transmission electron microscope at an accelerate voltage of 200 kV.

The dispersion of platinum in different catalysts was determined by  $\text{H}_2$  pulse adsorption on a chemisorption analyzer (Chemisorb 2720, Micromeritics). In a typical experiment, *ca.* 100 mg sample in the quartz reactor was pre-oxidized in  $\text{O}_2/\text{He}$  at 400 °C for 1 h to ensure removal of hydrocarbons on the surface and then cooled to room temperature in flowing He. Subsequently, the sample was heated in 5% $\text{H}_2/\text{Ar}$  to 350 °C, reduced in 5% $\text{H}_2/\text{Ar}$  at 350 °C for 1 h and then treated in He at 350 °C until no hydrogen desorption can be observed. The possible hydrogen spillover is believed to be elim-

inated. After cooling down to room temperature in flowing He, pulses of  $\text{H}_2$  were injected to the reactor every 1 min until no further changes in intensity of outlet  $\text{H}_2$  (*ca.* 20 min). The dispersion of platinum was calculated assuming the equimolar adsorption of H on platinum.

The  $^{27}\text{Al}$  MAS-NMR spectra were recorded on a Bruker DRX400 spectrometer (9.4T). The samples were spun in the rotors. The r.f. pulse with the length of 0.3  $\mu\text{s}$  was applied and the MAS frequency was fixed at 20 kHz. The spectrum was acquired after 2000 accumulations with the acquisition time of 0.1 s. A time interval of 1 s was selected between two successive accumulations to avoid saturation effects. Saturated  $\text{Al}(\text{NO}_3)_3$  solution was used as the  $^{27}\text{Al}$  chemical shift reference.

The acidity of Si-MCM-41 and Al-MCM-41 was determined by FT-IR spectra of pyridine adsorption. Prior to pyridine adsorption, the sample of *ca.* 0.1 g was out gassed at 400 °C for 2 h and cooled down to room temperature under vacuum. Pyridine was then introduced to the sample at saturated vapor pressure. Physisorbed pyridine was removed through heating the samples at 150 °C for 2 h and then the IR spectra were recorded. The bands in the IR spectra within the range of 1512–1567  $\text{cm}^{-1}$  are corresponding to the Brønsted acid sites [17].

## 2.3. Catalytic testing

The selective catalytic reduction of NO by hydrogen at atmospheric pressure was carried out in a fixed-bed flow microreactor. The typical reactant gas composition was NO (1000 ppm),  $\text{H}_2$  (5000 ppm),  $\text{O}_2$  (6.7%), and the balance He. The total flow of the inlet gas was set at 200  $\text{mL min}^{-1}$ . A sample weight of 100 mg was employed, corresponding to the gas hourly space velocity (GHSV) of 80,000  $\text{h}^{-1}$ . Prior to testing, the samples were pretreated in  $\text{O}_2/\text{He}$  (6.7%  $\text{O}_2$ , 100  $\text{mL min}^{-1}$ ) for 1 h at 400 °C. The products were analyzed on-line using a gas chromatograph (HP 6820 series, for  $\text{N}_2$  and  $\text{N}_2\text{O}$  analysis) and a chemiluminescence  $\text{NO}_x$  analyzer (Ecotech EC 9841, for NO and  $\text{NO}_2$  analysis). The nitrogen balance is calculated for each step using the following equation, where  $\text{NO}_x$  is the sum of NO and  $\text{NO}_2$ :  $[\text{NO}_x]_{\text{inlet}} = [\text{NO}_x]_{\text{outlet}} + 2[\text{N}_2\text{O}]_{\text{outlet}} + 2[\text{N}_2]_{\text{outlet}}$ . This N-balance was found to be >95% for all experiments. The  $\text{NO}_x$  conversion is calculated as  $X\text{NO}_x = ([\text{NO}_x]_{\text{inlet}} - [\text{NO}_x]_{\text{outlet}})/[\text{NO}_x]_{\text{inlet}}$ . The  $\text{N}_2$  selectivity is calculated as  $S_{\text{N}_2} = 2 \times [\text{N}_2]/([\text{NO}_x]_{\text{inlet}} -$

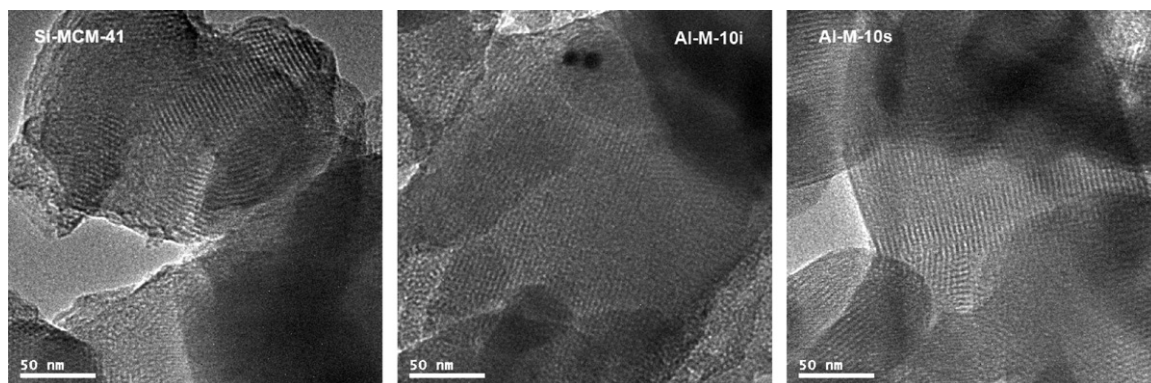


Fig. 2. TEM images of Si-MCM-41, Al-M-10i and Al-M-10s.

**Table 1**  
Pore structural parameters and Brønsted acidity of Al-MCM-41 samples.

Sample	$S_{\text{BET}}$ ( $\text{m}^2/\text{g}$ )	Pore diameter (nm)	Pore volume ( $\text{cm}^3/\text{g}$ )	Brønsted acid (mmol/g)
Si-MCM-41	1097	3.21	0.91	–
Al-M-80i	896	2.97	0.66	0.06
Al-M-40i	861	2.96	0.64	0.11
Al-M-20i	827	2.94	0.61	0.16
Al-M-10i	755	2.92	0.56	0.26
Al-M-5i	700	2.85	0.51	0.29
Al-M-80s	952	3.62	0.83	0.09
Al-M-40s	728	3.86	0.73	0.14
Al-M-20s	600	3.96	0.70	0.20
Al-M-10s	542	4.58	0.64	0.33
Al-M-5s	426	4.55	0.48	0.38

$[\text{NO}_x]_{\text{outlet}}$ ), and the  $\text{N}_2\text{O}$  selectivity is calculated as  $S_{\text{N}_2\text{O}} = 2 \times [\text{N}_2\text{O}] / ([\text{NO}_x]_{\text{inlet}} - [\text{NO}_x]_{\text{outlet}})$ .

#### 2.4. In situ DRIFT study for $\text{H}_2$ -SCR

In situ DRIFT spectra were recorded on the Bruker Tensor 27 spectrometer, equipped with a liquid  $\text{N}_2$  cooled high sensitivity MCT detector. The catalyst samples of ca. 25 mg were finely ground and placed in the chamber. Prior to each experiment, the samples were pretreated in  $\text{O}_2/\text{He}$  at  $400^\circ\text{C}$  for 1 h, and cooled to the desired temperature for taking a reference spectrum. Then, the reaction gas mixture (1000 ppm NO, 5000 ppm  $\text{H}_2$ , 6.7%  $\text{O}_2$ , He balance, 25 mL/min) was fed and the steady-state spectra were recorded with a resolution of  $4\text{ cm}^{-1}$  and an accumulation of 128 scans.

### 3. Results and discussion

#### 3.1. Characterization of Al-MCM-41

Fig. 1 shows the XRD patterns of Al-MCM-41 samples prepared by different methods. For Al-MCM-41 prepared by wet impregnation, three diffraction peaks at  $2\theta = 2.1^\circ$ ,  $3.8^\circ$  and  $4.4^\circ$  are clearly observed on all samples, indexed as (1 0 0), (1 1 0) and (2 0 0) diffraction peak of characteristic MCM-41 structure respectively [18]. With increasing Al loadings, i.e. decreasing Si/Al ratios from 80 to 5, only slight decreases in peak intensities are observed, indicating that the hexagonally order structure are well preserved with the introduction of Al species by wet impregnation. For Al-MCM-41 prepared by isomorphous substitution, three diffraction peaks at  $2\theta = 2.1^\circ$ ,  $3.8^\circ$  and  $4.4^\circ$  are observed at low Al loadings, i.e. Si/Al = 80 and 40. With increasing Al loadings, the intensity of (1 0 0) diffraction peak decreases while the (1 1 0) and (2 0 0) diffraction peaks gradually disappear. Obviously, substitution of framework  $\text{Si}^{4+}$  by

$\text{Al}^{3+}$  in MCM-41 may result in the partially destruction of hexagonally order structure.

The textural properties of Al-MCM-41 samples are characterized and the results are summarized in Table 1. It is seen that the introduction of Al species to Si-MCM-41 results in general decreases in the specific surface areas. For Al-MCM-41 prepared by wet impregnation, both the pore diameters and pore volumes gradually decrease as Al loadings increase. For Al-MCM-41 prepared by isomorphous substitution, the pore diameters gradually increase as Al loadings increase (Si/Al ratios decrease from 80 to 10) while the pore volumes decrease probably due to the partially destruction of mesoporous structure as revealed in XRD patterns. The worm-like morphology consisting of mesopores are clearly observed on Si-MCM-41 and Al-MCM-41 at Si/Al = 10, as indicated by the TEM images in Fig. 2.

Introduction of Al species to MCM-41 by wet impregnation or isomorphous substitution results in the appearance of Brønsted acid sites and higher amount of Brønsted acid sites are observed with higher Al loadings, as indicated by the data in Table 1. It is also seen that more Brønsted acid sites are created in Al-MCM-41 sample prepared by isomorphous substi-

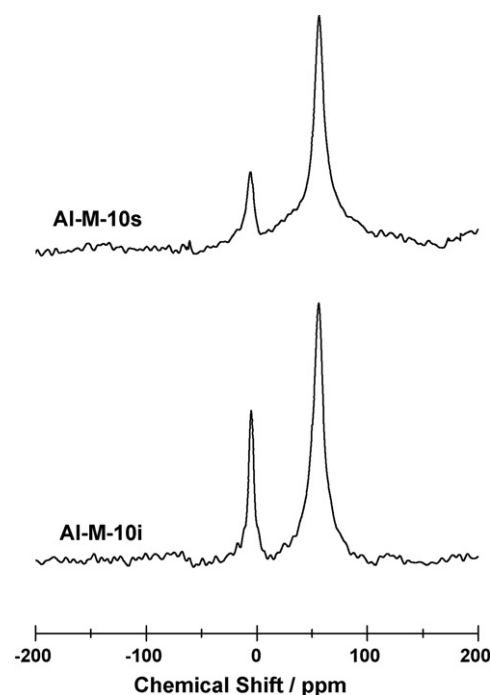


Fig. 3.  $^{27}\text{Al}$  MAS-NMR spectra of Al-M-10i and Al-M-10s.

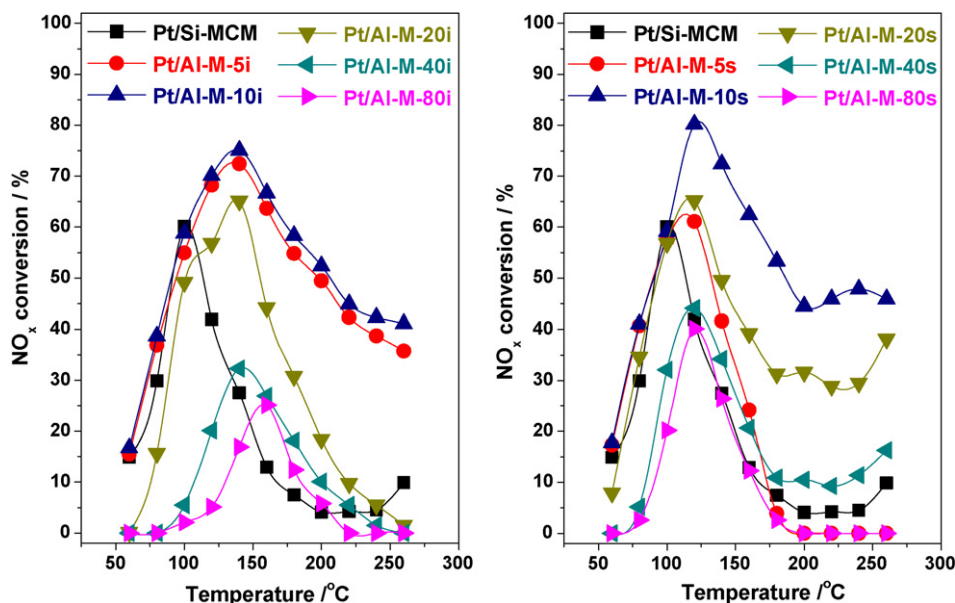


Fig. 4. Catalytic activities for H<sub>2</sub>-SCR on Pt/Si-MCM-41 and Pt/Al-MCM-41. Reaction conditions: NO = 1000 ppm, H<sub>2</sub> = 5000 ppm, O<sub>2</sub> = 6.7%, He balance, GHSV = 80,000 h<sup>-1</sup>.

tution than that prepared by wet impregnation with similar Al loading.

The <sup>27</sup>Al MAS-NMR spectra provide useful information regarding the coordination of aluminum in Al-MCM-41. As seen in Fig. 3, two types of aluminum are observed in Al-MCM-41 at Si/Al = 10: tetrahedrally coordinated Al in the framework at *ca.* 53 ppm and framework-connected octahedral Al species at *ca.* 0 ppm [19]. It is clearly indicated that not all the aluminum species are in the framework of MCM-41 and some aluminum may exist in the form of bulk Al<sub>2</sub>O<sub>3</sub> connecting with the framework. As is known, Al species in the framework are the origin of Brønsted acid sites in Al-MCM-41. More framework Al species are observed in Al-MCM-41 sample prepared by isomorphous substitution than that prepared by wet impregnation at Si/Al = 10. And correspondingly, more Brønsted acid sites should be present in Al-M-10s than that in Al-M-10i, as proved by the data in Table 1.

Based on all above characterization results, it can be concluded that Al species can be introduced to the framework of MCM-41 by isomorphous substitution or wet impregnation and the meso-

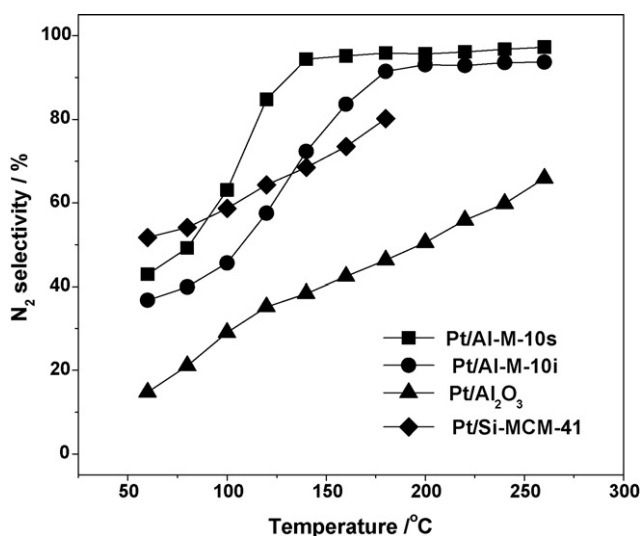


Fig. 5. N<sub>2</sub> selectivity during H<sub>2</sub>-SCR on different Pt catalysts. Reaction conditions: NO = 1000 ppm, H<sub>2</sub> = 5000 ppm, O<sub>2</sub> = 6.7%, He balance, GHSV = 80,000 h<sup>-1</sup>.

Table 2  
Pt loadings and Pt dispersion in different Pt catalysts.

Catalyst	S <sub>BET</sub> (m <sup>2</sup> /g)	Pt loading (%) <sup>a</sup>	Pt dispersion (%) <sup>b</sup>
Pt/Si-MCM-41	1029	0.93	39.7
Pt/Al-M-80i	877	0.97	42.4
Pt/Al-M-40i	858	0.94	44.5
Pt/Al-M-20i	801	0.96	48.7
Pt/Al-M-10i	739	0.92	53.1
Pt/Al-M-5i	682	0.97	58.6
Pt/Al-M-80s	943	0.94	40.4
Pt/Al-M-40s	706	0.95	41.9
Pt/Al-M-20s	587	0.91	45.7
Pt/Al-M-10s	538	0.94	49.2
Pt/Al-M-5s	419	0.92	51.9

<sup>a</sup> Determined by ICP.

<sup>b</sup> Determined by H<sub>2</sub> chemisorption.

porous structure can be well preserved at certain Si/Al ratios. Brønsted acid sites are created due to the introduction of framework Al species and more Brønsted acid sites are observed on Al-MCM-41 prepared by isomorphous substitution than that prepared by wet impregnation with similar Al loading.

After the impregnation of Pt, the surface areas of mesoporous support materials decrease slightly (within 5%), as seen in Table 2. The exact Pt loadings in Pt catalysts are determined to be in the range of 0.91–0.97%, very much close to the theoretic value of 1%. Moreover, after the introduction of Al species to MCM-41 supports, the Pt dispersion increases to some extent. Typically, the Pt dispersion increases from 39.7% in Pt/Si-MCM-41 to 58.6% in Pt/Al-M-5i, while it increases to 51.9% in Pt/Al-M-5s.

### 3.2. Catalytic performance of Pt/Al-MCM-41

The catalytic activities for H<sub>2</sub>-SCR over Pt/Si-MCM-41 and Pt/Al-MCM-41 are shown in Fig. 4. It is seen that the introduction of Al species to MCM-41 support shows obvious effects on NO<sub>x</sub> conversion, which are dependent on the preparation methods of Al-MCM-41 and Si/Al ratios. Generally, promotion effect is observed at relative high Al loadings, *i.e.* Si/Al ratios < 20. For Pt/Al-M-xi, the catalytic activity increases as Si/Al ratios decrease from 80 to 10 and the catalytic activity decreases slightly as Si/Al ratio further decreases to 5. The highest NO<sub>x</sub> conversion of *ca.* 75% is obtained on Pt/Al-M-10i at 140 °C. For Pt/Al-M-xs, the catalytic activity also

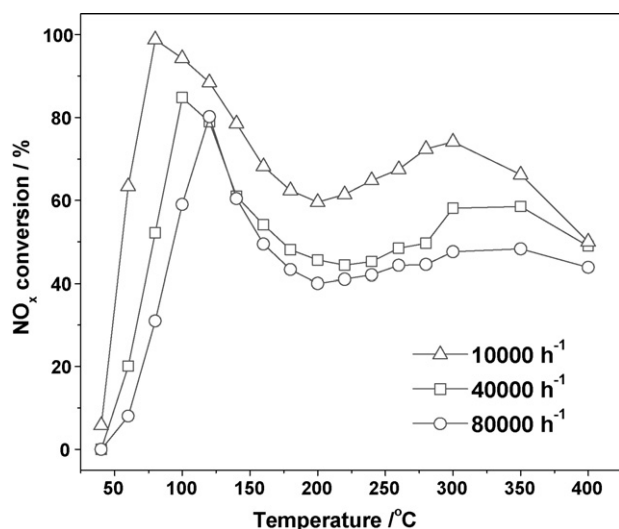


Fig. 6. Effect of GHSV on  $\text{NO}_x$  conversion over Pt/Al-M-10s. Reaction conditions:  $\text{NO} = 1000$  ppm,  $\text{H}_2 = 5000$  ppm,  $\text{O}_2 = 6.7\%$ , He balance.

increases as Si/Al ratios decrease from 80 to 10, while a dramatic decrease is observed as Si/Al ratio further decreases to 5. The highest  $\text{NO}_x$  conversion of ca. 80% is obtained on Pt/Al-M-10s at  $120^\circ\text{C}$ . The low activity of Pt/Al-M-5s is presumably ascribed to the serious destruction of mesoporous structure, as indicated by XRD and low temperature  $\text{N}_2$  adsorption/desorption results.

The  $\text{N}_2$  selectivity during  $\text{H}_2$ -SCR over several Pt catalysts is displayed in Fig. 5. The  $\text{N}_2$  selectivity over Pt/ $\text{Al}_2\text{O}_3$  is rather low at low temperatures, but it gradually increases with increasing temperatures. In contrast,  $\text{N}_2$  selectivity of 50–80% can be obtained on Pt/Si-MCM-41 in the temperature range of  $60$ – $160^\circ\text{C}$ . The introduction of Al species to MCM-41 results in the enhancement of  $\text{N}_2$  selectivity at high temperatures. For Pt/Al-MCM-41 at Si/Al = 10,  $\text{N}_2$

selectivity of ca. 40% is observed at  $60^\circ\text{C}$  and it gradually increases to >90% with increasing temperatures. It is also seen that Pt/Al-M-10s shows higher  $\text{N}_2$  selectivity than Pt/Al-M-10i in the whole temperature range studied. As indicated by NMR results, more bulk  $\text{Al}_2\text{O}_3$  are present in Pt/Al-M-10i, and hence more Pt species may locate on the  $\text{Al}_2\text{O}_3$  to form Pt/ $\text{Al}_2\text{O}_3$  instead of locating on the mesoporous structure of Al-MCM-41. Since the  $\text{N}_2$  selectivity on Pt/ $\text{Al}_2\text{O}_3$  is rather low, the  $\text{N}_2$  selectivity on Pt/Al-M-10i is thus lower than that on Pt/Al-M-10s.

As indicated by the catalytic results, the introduction of Al species to Si-MCM-41 at certain Si/Al ratios shows significant promotion effect on  $\text{H}_2$ -SCR over Pt/MCM-41. The promotion effect is observed not only in the catalytic activity but also in the  $\text{N}_2$  selectivity. Among all Pt/Al-MCM-41 catalysts studied, Pt/Al-M-10s shows the best catalytic performance and a maximal  $\text{NO}_x$  conversion of ca. 80% can be obtained at  $120^\circ\text{C}$  when  $\text{N}_2$  selectivity is as high as ca. 85%. It has been reported that surface acidity produced by Al species can greatly improve the activity of Pt/MCM-41 for HC-SCR reaction [20]. In this study, similar results are obtained on Pt/MCM-41 for  $\text{H}_2$ -SCR reaction and the functions of acid sites will be discussed integrated with in situ DRIFT results in the following section.

The effects of GHSV on  $\text{NO}_x$  conversion over the best catalyst Pt/Al-M-10s are shown in Fig. 6. It is seen that  $\text{NO}_x$  conversion increases with decreasing GHSV from 80,000 to  $10,000\text{ h}^{-1}$ . Meanwhile, the temperature when maximal  $\text{NO}_x$  conversion is achieved shifts to lower temperatures. At low GHSV of  $10,000\text{ h}^{-1}$ , an overall  $\text{NO}_x$  conversion can be obtained at  $80^\circ\text{C}$ .

### 3.3. In situ DRIFT study on $\text{H}_2$ -SCR

In situ DRIFT spectra obtained under  $\text{NO-H}_2\text{-O}_2$  reaction condition over Pt/Si-MCM-41 catalyst at various temperatures are shown in Fig. 7. Bands at 1840, 1755, 1625, 1585, 1420 and  $1370\text{ cm}^{-1}$  are observed and their intensities change with reaction temperatures. The band at  $1420\text{ cm}^{-1}$  is ascribed to adsorbed nitrites on support

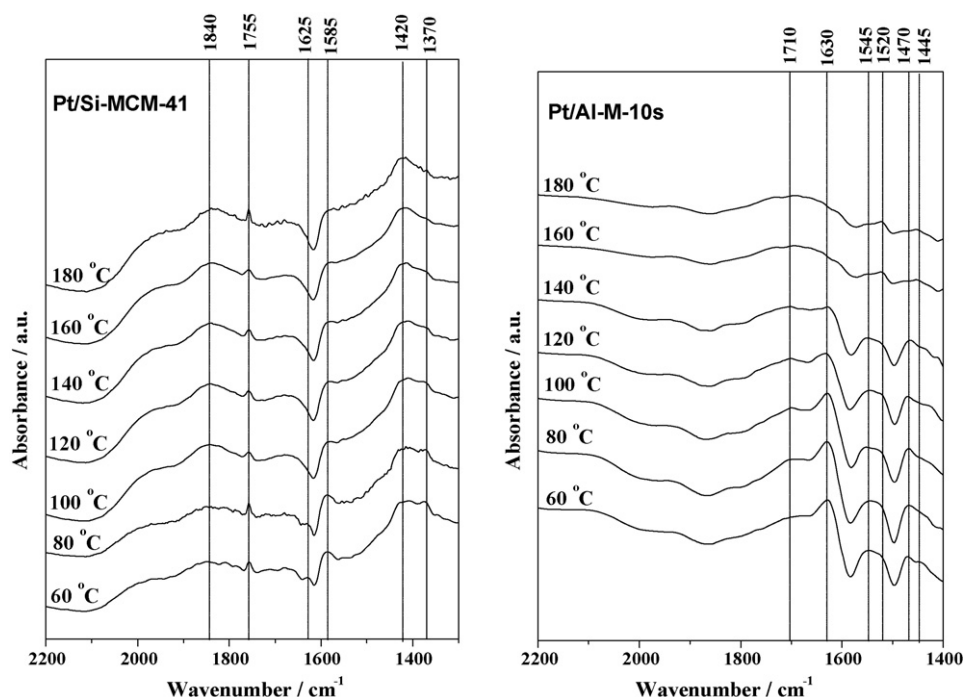


Fig. 7. In situ DRIFTS study of adsorbed species formed on Pt/Si-MCM-41 and Pt/Al-M-10s under  $\text{NO-H}_2\text{-O}_2$  reaction condition. Reaction conditions:  $\text{NO} = 1000$  ppm,  $\text{H}_2 = 5000$  ppm,  $\text{O}_2 = 6.7\%$ , He balance.

[21] and the band at  $1370\text{ cm}^{-1}$  is ascribed to free nitrates [22]. The bands at  $1625$  and  $1585\text{ cm}^{-1}$  are ascribed to bridging nitrates and chelating nitrates, respectively [23]. The band at  $1755\text{ cm}^{-1}$  is ascribed to linear NO on defects of Pt sites [24] while the band at  $1840\text{ cm}^{-1}$  is ascribed to mononitrosyl group on  $\text{Pt}^{\text{II}}$  [25]. Based on above observations, the  $\text{H}_2$ -SCR pathway on Pt/Si-MCM-41 is proposed as following. In the initial step, gaseous NO adsorbs on the surface of Pt species as  $\text{NO}(\text{g}) + * \rightarrow -\text{NO}$  (\*: active sites). Adsorbed NO may dissociate ( $-\text{NO} + * \rightarrow -\text{N} + -\text{O}$ ) and recombine to produce  $\text{N}_2$  ( $-\text{N} + -\text{N} \rightarrow \text{N}_2 + 2*$ ) and by-product  $\text{N}_2\text{O}$  ( $-\text{N} + -\text{NO} \rightarrow \text{N}_2\text{O} + 2*$ ), as proposed by Burch et al. [26]. Meanwhile, the adsorbed NO species are oxidized to adsorbed nitrites or nitrates and then store on the support, as observed in the DRIFT spectra. These nitrites and nitrates may be reduced by hydrogen to produce  $\text{N}_2$  or  $\text{N}_2\text{O}$  with different reactivity.

With the introduction of Al species to Si-MCM-41 by isomorphous substitution, i.e. the introduction of Brønsted acid sites, the adsorbed species on catalysts change greatly and bands at  $1710$ ,  $1630$ ,  $1545$ ,  $1520$ ,  $1470$  and  $1445\text{ cm}^{-1}$  are observed on Pt/Al-M-10s. The band at  $1710\text{ cm}^{-1}$  is ascribed to linear NO species on the terrace sites of Pt particles [24]. The band at  $1630\text{ cm}^{-1}$  is ascribed to bridging nitrates while the bands at  $1545$  and  $1520\text{ cm}^{-1}$  are ascribed to monodentate nitrates [25]. Remarkably, bands at  $1470$  and  $1445\text{ cm}^{-1}$  corresponding to  $\text{NH}_4^+$  on Brønsted acid sites [7,11] are observed. The  $\text{NH}_4^+$  is key reaction intermediate for  $\text{NH}_3$ -SCR with high reactivity, as suggested by Richter et al. [27]. Based on the in situ DRIFT spectra and catalytic results, a different  $\text{H}_2$ -SCR reaction pathway is proposed for Pt/Al-MCM-41 with Brønsted acid sites. In the initial step, gaseous NO adsorbs as linear NO species on the terrace sites of Pt particles:  $\text{NO} + * \rightarrow -\text{NO}$ . The adsorbed NO species easily dissociate to produced adsorbed N and adsorbed O ( $-\text{NO} + * \rightarrow -\text{N} + -\text{O}$ ), motivated by the low reaction barrier [28]. The dissociation of NO is also promoted by atomic hydrogen on Pt sites [29,30]. The adsorbed N may reacts with another adsorbed N to produce  $\text{N}_2$  ( $-\text{N} + -\text{N} \rightarrow \text{N}_2 + 2*$ ) and reacts with adsorbed NO to produce  $\text{N}_2\text{O}$  ( $-\text{N} + -\text{NO} \rightarrow \text{N}_2\text{O} + 2*$ ). This may be possible pathway for the formation of  $\text{N}_2$  and  $\text{N}_2\text{O}$  at low temperature, similar to that on Pt/Si-MCM-41. Alternatively, the adsorbed N may react with active hydrogen to produce  $-\text{NH}_3$  on Pt sites ( $-\text{N} + 3\text{H} \rightarrow -\text{NH}_3 + 3*$ ), which then migrate and store on the Brønsted acid sites as observed in the DRIFT spectra. The  $\text{NH}_4^+$  species react with gaseous NO and  $\text{O}_2$  to produce  $\text{N}_2$  and  $\text{H}_2\text{O}$  with high reactivity and selectivity ( $4-\text{NH}_4^+ + 4\text{NO} + \text{O}_2 \rightarrow 4\text{N}_2 + 6\text{H}_2\text{O} + -\text{H}^+$ ). This is another possible pathway for the formation of  $\text{N}_2$ . At relative lower temperatures,  $\text{N}_2$  and  $\text{N}_2\text{O}$  are observed as  $\text{H}_2$ -SCR products and both of the above-mentioned two reaction pathways may be involved. At relative higher temperatures,  $\text{N}_2$  is observed as the main  $\text{H}_2$ -SCR product and consequently the adsorbed  $\text{NH}_4^+$  should be the main reaction intermediates.

#### 4. Conclusion

By isomorphous substitution or wet impregnation, Al species can be introduced to MCM-41 at certain Si/Al ratio with the mesoporous structure well preserved. Some Al species exist in the form of framework Al species and others in the form of bulk  $\text{Al}_2\text{O}_3$ . Brønsted acid sites are created due to the introduction of framework Al species and more Brønsted acid sites are observed on Al-MCM-41 prepared by isomorphous substitution than that prepared by wet impregnation at similar Si/Al ratio. Al-MCM-41 with appropriate Brønsted acid sites appears to be better support for Pt than Si-MCM-41 for  $\text{H}_2$ -SCR reaction. A maximal  $\text{NO}_x$  conversion of ca. 80% with  $\text{N}_2$  selectivity of ca. 85% can be obtained at  $120^\circ\text{C}$  at high GHSV of  $80,000\text{ h}^{-1}$  over Pt/Al-MCM-41 prepared by isomorphous substitution at Si/Al ratio of 10. The introduction of

Brønsted acid sites changes the  $\text{H}_2$ -SCR reaction pathway and the  $\text{NH}_4^+$  species on Brønsted acid sites are observed as key intermediates for  $\text{N}_2$  production.

#### Acknowledgements

This work was financially supported National Natural Science Foundation of China (20973094, 20703057) and National Basic Research Program of China (2009CB623502). The support from International S&T Cooperation Program of China (ISCP) (2007DFA90720) is also greatly appreciated.

#### References

- [1] J.N. Armor, Environmental Catalysis, American Chemical Society, Washington, DC, 1994.
- [2] R. Burch, M.D. Coleman, An investigation of the  $\text{NO}/\text{H}_2/\text{O}_2$  reaction on noble-metal catalysts at low temperatures under lean-burn conditions, Appl. Catal. B 23 (1999) 115–121.
- [3] C.N. Costa, V.N. Stathopoulos, V.C. Belessi, A.M. Efstathiou, An investigation of the  $\text{NO}/\text{H}_2/\text{O}_2$  reaction on a highly active and selective Pt/La<sub>0.5</sub>Ce<sub>0.5</sub>MnO<sub>3</sub> Catalyst, J. Catal. 197 (2001) 350–364.
- [4] M. Machida, S. Ikeda, D. Kurogi, T. Kijima, Low temperature catalytic  $\text{NO}_x$ - $\text{H}_2$  reactions over Pt/TiO<sub>2</sub>-ZrO<sub>2</sub> in an excess oxygen, Appl. Catal. B 35 (2001) 107–116.
- [5] M. Machida, S. Ikeda, Oscillation in low-temperature  $\text{NO}-\text{H}_2-\text{O}_2$  reactions over Pt catalysts supported on  $\text{NO}_x$ -adsorbing material TiO<sub>2</sub>-ZrO<sub>2</sub>, J. Catal. 227 (2004) 53–59.
- [6] S. Hamada, K. Ikeue, M. Machida, Catalytic  $\text{NO}-\text{H}_2-\text{O}_2$  reaction over Pt/Mg-Al-O prepared from PtCl<sub>6</sub><sup>2-</sup> and Pt(NO<sub>2</sub>)<sub>4</sub><sup>2-</sup> exchanged hydrothermalites, Appl. Catal. B 71 (2006) 1–6.
- [7] J. Shibata, M. Hashimoto, K. Shimizu, H. Yoshida, T. Hattori, A. Satsuma, Factors controlling activity and selectivity for SCR of NO by hydrogen over supported platinum catalysts, J. Phys. Chem. B 108 (2004) 18327–18335.
- [8] M. Machida, T. Watanabe, Effect of Na-addition on catalytic activity of Pt-ZSM-5 for low-temperature  $\text{NO}-\text{H}_2-\text{O}_2$  reactions, Appl. Catal. B 52 (2004) 281–286.
- [9] C.N. Costa, A.M. Efstathiou, Low-temperature  $\text{H}_2$ -SCR of NO on a novel Pt/MgO-CeO<sub>2</sub> catalyst, Appl. Catal. B 72 (2007) 240–252.
- [10] M. Engelmann-Pirez, P. Granger, G. Leclercq, Investigation of the catalytic performances of supported noble metal based catalysts in the  $\text{NO} + \text{H}_2$  reaction under lean conditions, Catal. Today 107–108 (2005) 315–322.
- [11] G. Qi, R.T. Yang, F.C. Rinaldi, Selective catalytic reduction of nitric oxide with hydrogen over Pd-based catalysts, J. Catal. 237 (2006) 381–392.
- [12] L.D. Li, F.X. Zhang, N.J. Guan, E. Schreiber, M. Richter, NO selective reduction by hydrogen on potassium titanate supported palladium catalyst, Catal. Commun. 9 (2008) 1827–1832.
- [13] Y. Hasegawa, M. Haneda, Y. Kintaichi, H. Hamada, Zn-promoted Rh/SiO<sub>2</sub> catalyst for the selective reduction of NO with H<sub>2</sub> in the presence of O<sub>2</sub> and SO<sub>2</sub>, Appl. Catal. B 60 (2005) 41–47.
- [14] S.C. Shen, S. Kawi, Mechanism of selective catalytic reduction of NO in the presence of excess O<sub>2</sub> over Pt/Si-MCM-41 catalyst, J. Catal. 213 (2003) 241–250.
- [15] Y. Wan, J. Ma, Z. Wang, W. Zhou, S. Kaliaguine, Selective catalytic reduction of NO over Cu-Al-MCM-41, J. Catal. 227 (2004) 242–252.
- [16] P. Wu, Y.X. Liu, F.X. Zhang, L.D. Li, Y.L. Yang, N.J. Guan, Influences of mesoporous structure on the  $\text{NO} + \text{H}_2 + \text{O}_2$  low temperature reaction over Pt/Si-MCM-41 catalyst, Acta Phys. Chim. Sinica 24 (2008) 369–374.
- [17] R. Buzzoni, S. Bordiga, G. Ricchiardi, C. Lamberti, A. Zecchina, G. Bellussi, Interaction of pyridine with acidic and superacidic systems: an IR investigation, Langmuir 12 (1996) 930–940.
- [18] C.T. Kresge, M.E. Leonowicz, W.J. Roth, J.C. Vartuli, J.S. Beck, Ordered mesoporous molecular sieves synthesized by a liquid-crystal template mechanism, Nature 359 (1992) 710–712.
- [19] J.A. van Bokhoven, D.C. Koningsberger, P. Kunkeler, H. van Bekkum, A.P.M. Kentgens, Stepwise dealumination of zeolite beta at specific T-sites observed with <sup>27</sup>Al MAS and <sup>27</sup>Al MQ MAS NMR, J. Am. Chem. Soc. 122 (2000) 12842–12847.
- [20] S.C. Shen, S. Kawi, Selective catalytic reduction of NO by hydrocarbons in the presence of excess oxygen using Pt/MCM-41 catalysts, Appl. Catal. B 45 (2003) 63–76.
- [21] Y.Y. Ji, T.J. Hoops, U.M. Graham, G. Jacobs, M. Crocker, A kinetic and DRIFTS study of supported Pt catalysts for NO oxidation, Catal. Lett. 110 (2006) 29–37.
- [22] L.D. Li, L.L. Qu, J. Cheng, J.J. Li, Z.P. Hao, Oxidation of nitric oxide to nitrogen dioxide over Ru catalysts, Appl. Catal. B 88 (2009) 224–231.
- [23] K. Hadjiivanov, H. Knozinger, Species formed after NO adsorption and  $\text{NO} + \text{O}_2$  coadsorption on TiO<sub>2</sub>, Phys. Chem. Chem. Phys. 2 (2000) 2803–2806.
- [24] A. Bourane, O. Dulaurant, S. Salasc, C. Sarda, C. Bouly, D. Bianchi, Heats of adsorption of linear NO species on a Pt/Al<sub>2</sub>O<sub>3</sub> catalyst using in situ infrared spectroscopy under adsorption equilibrium, J. Catal. 204 (2001) 77–88.
- [25] K. Hadjiivanov, Identification of neutral and charged  $\text{N}_x\text{O}_y$  surface species by IR spectroscopy, Catal. Rev. Sci. Eng. 42 (2000) 71–144.
- [26] R. Burch, M.D. Coleman, An investigation of promoter effects in the reduction of NO by H<sub>2</sub> under lean-burn conditions, J. Catal. 208 (2002) 435–447.

- [27] M. Richter, R. Eckelt, B. Parlitz, R. Fricke, Low-temperature conversion of NO<sub>x</sub> to N<sub>2</sub> by zeolite-fixed ammonium ions, *Appl. Catal. B* 15 (1998) 129–146.
- [28] Z.P. Liu, J.J. Stephen, D.A. King, Step-enhanced selectivity of NO reduction on platinum-group metals, *J. Am. Chem. Soc.* 125 (2003) 14660–14661.
- [29] M. Uchida, A.T. Bell, A study of NO reduction by H<sub>2</sub> over an alumina-supported ruthenium catalyst, *J. Catal.* 60 (1979) 204–215.
- [30] W.C. Hecker, A.T. Bell, Reduction of NO by H<sub>2</sub> over silica-supported rhodium: infrared and kinetic studies, *J. Catal.* 92 (1985) 247–259.